

Original citation:

Mironov, O. A., Hassan, A. H. A., Morris, R. J. H. (Richard J. H.), Dobbie, A. (Andrew), Uhlarz, M., Chrastina, Daniel, Hague, J. P., Kiatgamolchai, S., Beanland, R., Gabani, S., Berkutov, I. B., Helm, Manfred, Drachenko, O., Myronov, Maksym and Leadley, D. R. (David R.). (2014) Ultra high hole mobilities in a pure strained Ge quantum well. Thin Solid Films, Volume 557 . pp. 329-333.

Permanent WRAP url:

<http://wrap.warwick.ac.uk/62962>

Copyright and reuse:

The Warwick Research Archive Portal (WRAP) makes this work of researchers of the University of Warwick available open access under the following conditions.

This article is made available under the Creative Commons Attribution- 3.0 Unported (CC BY 3.0) license and may be reused according to the conditions of the license. For more details see <http://creativecommons.org/licenses/by/3.0/>

A note on versions:

The version presented in WRAP is the published version, or, version of record, and may be cited as it appears here.

For more information, please contact the WRAP Team at: publications@warwick.ac.uk



Ultra high hole mobilities in a pure strained Ge quantum well



O.A. Mironov^{a,b,1}, A.H.A. Hassan^{a,j,1,*}, R.J.H. Morris^{a,1}, A. Dobbie^{a,1}, M. Uhlarz^c, D. Chrastina^d, J.P. Hague^e, S. Kiatgamolchai^f, R. Beanland^{a,1}, S. Gabani^g, I.B. Berkutov^h, M. Helmⁱ, O. Drachenkoⁱ, M. Myronov^{a,1}, D.R. Leadley^{a,1}

^a Department of Physics, University of Warwick, Coventry CV4 7AL, UK

^b International Laboratory of High Magnetic Fields and Low Temperatures, 53-421 Wrocław, Poland

^c High Magnetic Field Laboratory, Helmholtz-Zentrum Dresden-Rossendorf, 01328 Dresden, Germany

^d L-NESS Politecnico di Milano, Polo di Como, Via Anzani 42, 22100 Como, Italy

^e Department of Physical Sciences, The Open University, Walton Hall, Milton Keynes MK7 6AA, UK

^f Department of Physics, Faculty of Science, Chulalongkorn University, 254 Phayathai Road, Pathumwan, Bangkok 10330, Thailand

^g Centre of Low Temperature Physics, Institute of Experimental Physics SAS, Košice, Slovakia

^h B.I. Verkin Institute for Low Temperature Physics and Engineering of NAS of Ukraine, Kharkov, Ukraine

ⁱ Institute of Ion Beam Physics and Materials Research, Helmholtz-Zentrum Dresden-Rossendorf, 01328 Dresden, Germany

^j Department of Physics, Tripoli University, Tripoli, Libya

ARTICLE INFO

Available online 29 October 2013

Keywords:
Strained Ge
ME-MSA
BAMS
Drift mobility
Ge QW channel

ABSTRACT

Hole mobilities at low and room temperature (RT) have been studied for a strained sGe/SiGe heterostructure using standard Van der Pauw resistivity and Hall effect measurements. The range of magnetic field and temperatures used were $-14\text{ T} < B < +14\text{ T}$ and $1.5\text{ K} < T < 300\text{ K}$ respectively. Using maximum entropy-mobility spectrum analysis (ME-MSA) and Bryan's algorithm mobility spectrum (BAMS) analysis, a RT two dimensional hole gas drift mobility of $(3.9 \pm 0.4) \times 10^3\text{ cm}^2/\text{V s}$ was determined for a sheet density (p_s) $9.8 \times 10^{10}\text{ cm}^{-2}$ (by ME-MSA) and $(3.9 \pm 0.2) \times 10^3\text{ cm}^2/\text{V s}$ for a sheet density (p_s) $5.9 \times 10^{10}\text{ cm}^{-2}$ (by BAMS).

© 2013 The Authors. Published by Elsevier B.V. This is an open access article under the CC BY license (<http://creativecommons.org/licenses/by/3.0/>).

1. Introduction

The transport properties of the two dimensional hole gas in a strained Ge (sGe) quantum well (QW) have been the focus of intensive research for many years because of its potential for device applications. Both low temperature (LT) [1–5] and room temperature (RT) [6–15] measurements have been studied in order to obtain a better understanding of the fundamental physics behind these transport properties. It is found that to obtain an improved electrical performance for sGe, a high purity Ge QW needs to be grown on a Ge-rich buffer layer with a low defect density. Hole mobilities at RT of up to $3000\text{ cm}^2/\text{V s}$ [6–13] have been reported for structures grown via low-energy plasma-enhanced chemical vapor deposition (LEPE-CVD) [12,14] and solid source molecular beam epitaxy (SS-MBE) [9,13]. However, growth by reduced pressure chemical vapor deposition (RP-CVD) utilizing a low growth temperature methodology has enabled a pure sGe QW (Si concentration less than 0.01 at.%) with monolayer precision [16] to be

grown, leading to the highest reported hole mobility to date for sGe at 10 K ($1.1 \times 10^6\text{ cm}^2/\text{V s}$ at a sheet density of $3 \times 10^{11}\text{ cm}^{-2}$) [1]. In this work we present further analysis and results using mobility spectrum analysis to extract the RT mobility for this sample. Historically, the first mobility spectrum analysis for a “pure germanium” [17] sample revealed a hole mobility of $1665\text{ cm}^2/\text{V s}$. However, the sGe QW composition for these samples was subsequently determined to be ~95% Ge, i.e. ~5% of Si was present in the QW which acts as an extra scattering center [18]. Theory predicts that at RT the hole mobility for pure Ge could be as high as $5000\text{ cm}^2/\text{V s}$ [7], a value considered possible for the present structure given it has the highest low temperature mobility reported in the literature to date. However, the directly measured RT hole mobility from Hall effect measurements is just $1347\text{ cm}^2/\text{V s}$, but this value represents the mean hole mobility from all parallel conducting layers, including the buffer and dopant supply layer as well as the sGe channel.

The RT hole mobility was determined using two independent mobility spectrum methods, maximum entropy-mobility spectrum analysis (ME-MSA) [19] and Bryan's algorithm mobility spectrum (BAMS) [20] technique. Both methods use the magnetoconductivity tensor as experimentally obtained over the wide magnetic field range of $-14\text{ T} < B < +14\text{ T}$, and a RT mobility of $(3.9 \pm 0.2) \times 1000\text{ cm}^2/\text{V s}$ (BAMS) and $(3.9 \pm 0.4) \times 1000\text{ cm}^2/\text{V s}$ (ME-MSA) were determined.

* Corresponding author.

E-mail address: OAMironov@yahoo.co.uk (O.A. Mironov).

¹ Tel.: +44 787 615 7335; fax: +44 2476 692016.

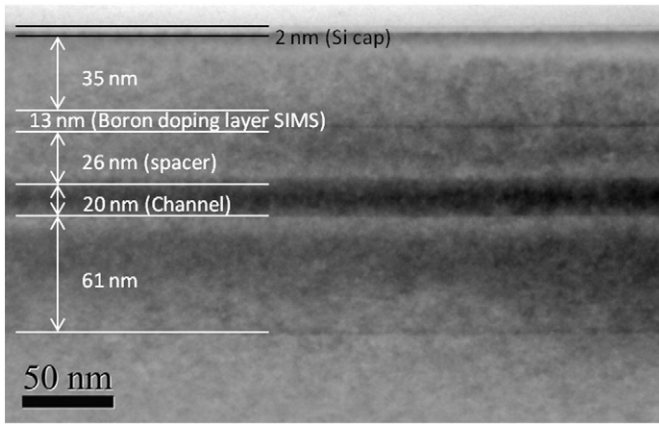


Fig. 1. Dark field (004) cross sectional transmission electron microscope image showing the various layers (highlighted) of sample 11-289.

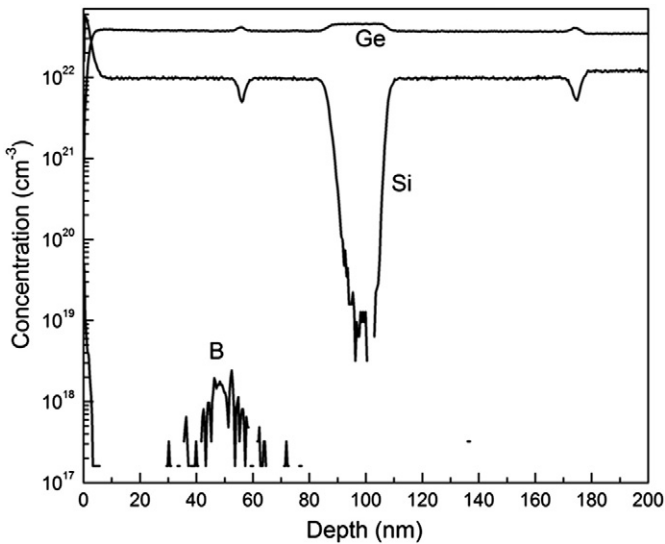


Fig. 2. B, Si and Ge uleSIMS depth profile for the sGe/SiGe heterostructure 11-289.

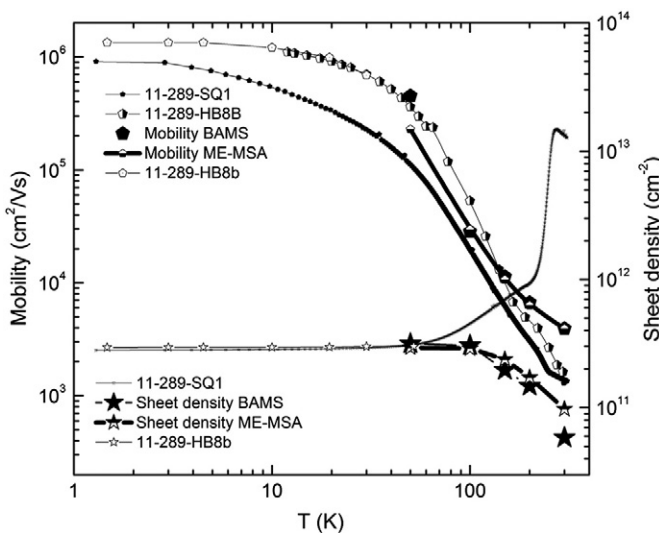


Fig. 3. Hall mobility and carrier sheet density of the Van der Pauw square (11-289-SQ1) and the Hall bar (11-289-HB8B) samples, compared to ME-MSA and BAMS results.

2. Results and discussion

2.1. Sample structure and measurement procedures

The normally-doped heterostructure used for this study is shown in Fig. 1 and contains a 20 ± 1.0 nm sGe QW on top of a $\text{Si}_{0.2}\text{Ge}_{0.8}$ reverse-graded buffer grown at 850 °C on a 100 mm diameter Si (001) substrate [21,22] using an ASM Epsilon 2000 RP-CVD reactor. A 13 nm boron doping layer (observed by ultra low energy secondary ion mass spectrometry (uleSIMS)) was grown above the channel and is separated by a 26 ± 1.0 nm $\text{Si}_{0.2}\text{Ge}_{0.8}$ spacer layer, while the structure was completed by a 44 ± 2.0 nm $\text{Si}_{0.2}\text{Ge}_{0.8}$ layer and a 2 ± 1.0 nm Si cap all grown at 500 °C to avoid subsequent strain relaxation of the Ge channel [23]. The in-plane strain was determined to be 0.65% with respect to the underlying $\text{Si}_{0.2}\text{Ge}_{0.8}$ buffer using X-ray diffraction [1,24], and was also used to confirm that the channel thickness was 20 ± 1.0 nm. The uleSIMS depth profile (Fig. 2) shows all the quantified layer concentrations and thicknesses [25].

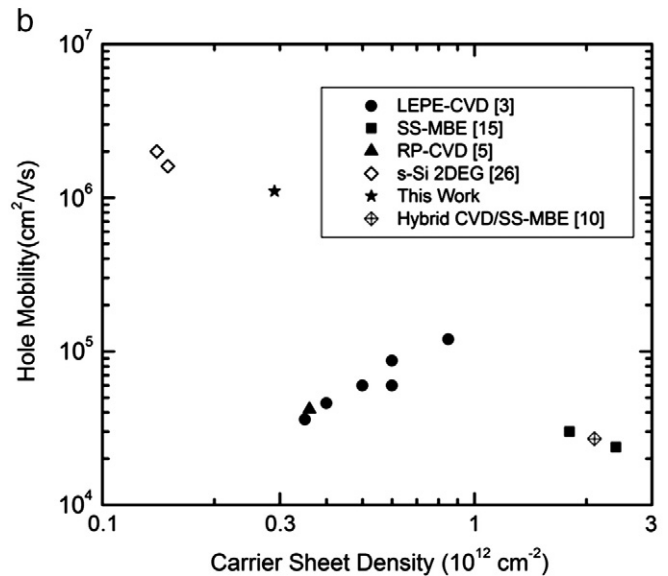
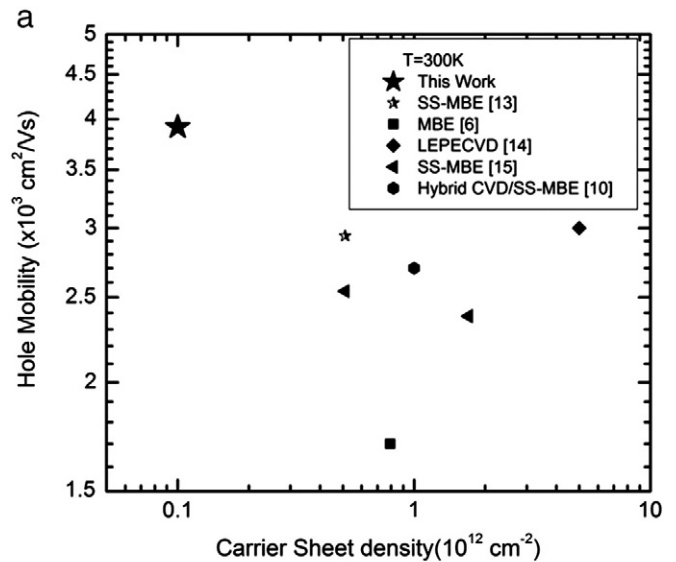


Fig. 4. Mobility comparison for different growth methods at (a) room temperature, and (b) low temperature, reported in literature.

2.2. Measurement analysis and ME-MSA method

Magnetotransport measurements were performed on a 4×4 mm square Van der Pauw sample (11-289-SQ1). Al contacts positioned at the sample corners were thermally evaporated prior to annealing at 425°C for 20 min under dry N_2 in order to produce needle-like penetration to a depth of $\sim 60\text{--}120$ nm and form ohmic contacts. The measured Hall mobility is shown in Fig. 3 as a function of temperature. A hole mobility of $9.08 \times 10^5 \text{ cm}^2/\text{Vs}$ with a carrier sheet density of $p_s = 2.79 \times 10^{11} \text{ cm}^{-2}$ was observed at 1.5 K, which is the highest LT hole mobility to date for sGe measured using the Van der Pauw configuration. However, it is less than the values previously measured using the Hall bar (HB) geometry for this sample (11-289-HB8B) [1]. This difference may be a consequence of the two samples being from different parts of the wafer which itself may not be completely homogenous, or because they are measured using different device geometries. Further studies are required to determine the source of this variation.

The measured RT Hall mobility of our sample (Fig. 3) was $1347 \text{ cm}^2/\text{Vs}$ while the combined layer sheet density i.e. at RT all conducting layers contribute to the mobility and carrier density, was $p_s^* = \frac{1}{eR_H} = 1.27 \times 10^{13} \text{ cm}^{-2}$, where R_H is the measured Hall coefficient and e the electron charge.

Fig. 4a illustrates a comparison of the mobility at RT while Fig. 4b shows the comparison of the Hall mobility at low temperature (4 K–20 K) for various sGe QWs grown by SS-MBE, LEPE-CVD and RP-CVD, as well as the highest electron mobility recorded for a strained silicon heterostructure [26].

Using ME-MSA [19] we extracted the sGe channel drift mobility and sheet density from 50 K up to RT (Fig. 5). The calculated mobilities and sheet densities are also shown in Fig. 3 alongside the Hall effect data, and are found to be extremely comparable. At RT a ME-MSA mobility of $(3.9 \pm 0.4) \times 1000 \text{ cm}^2/\text{Vs}$ ($p_s = 9.8 \times 10^{10} \text{ cm}^{-2}$) was determined and is the highest RT drift mobility published to date (Fig. 4). However, given the correspondingly low sheet density, the channel represents only 2–4% of the overall sample conductivity if all parallel layers are considered. Moreover, this RT channel carrier density is lower than

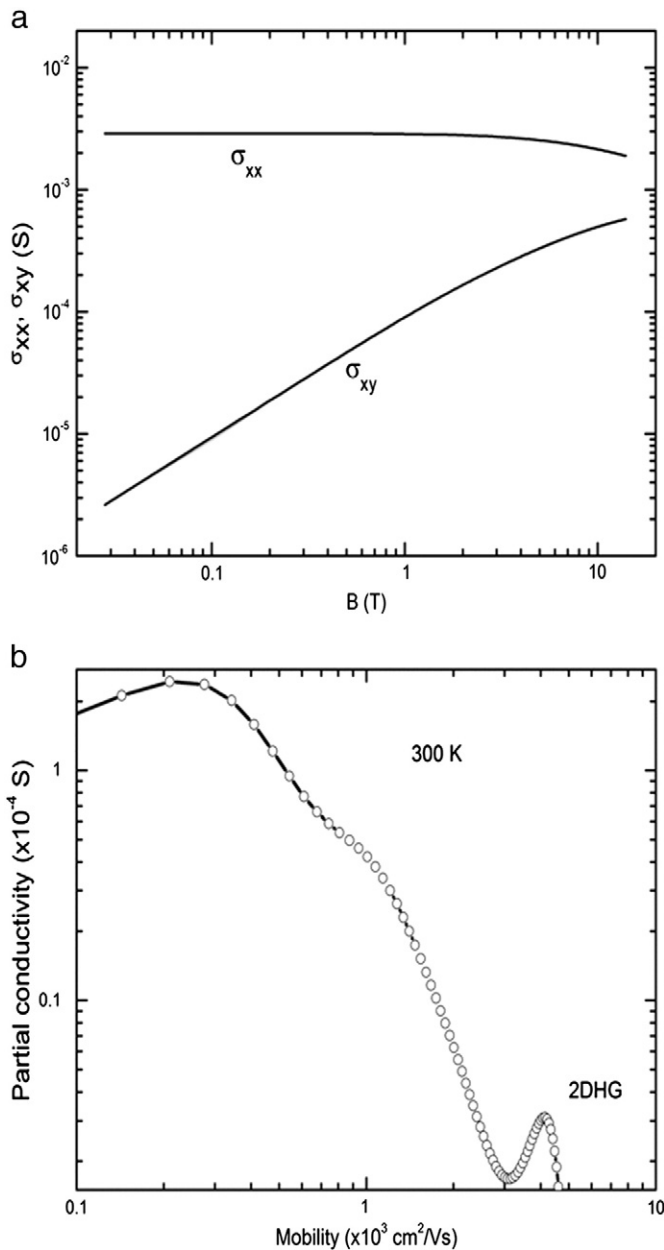


Fig. 5. (a) Magnetoconductivity σ_{xx} and σ_{xy} as function of magnetic field (B) for 11-289-SQ1 and (b) mobility spectrum at 300 K using the ME-MSA approach for 11-289-SQ1.

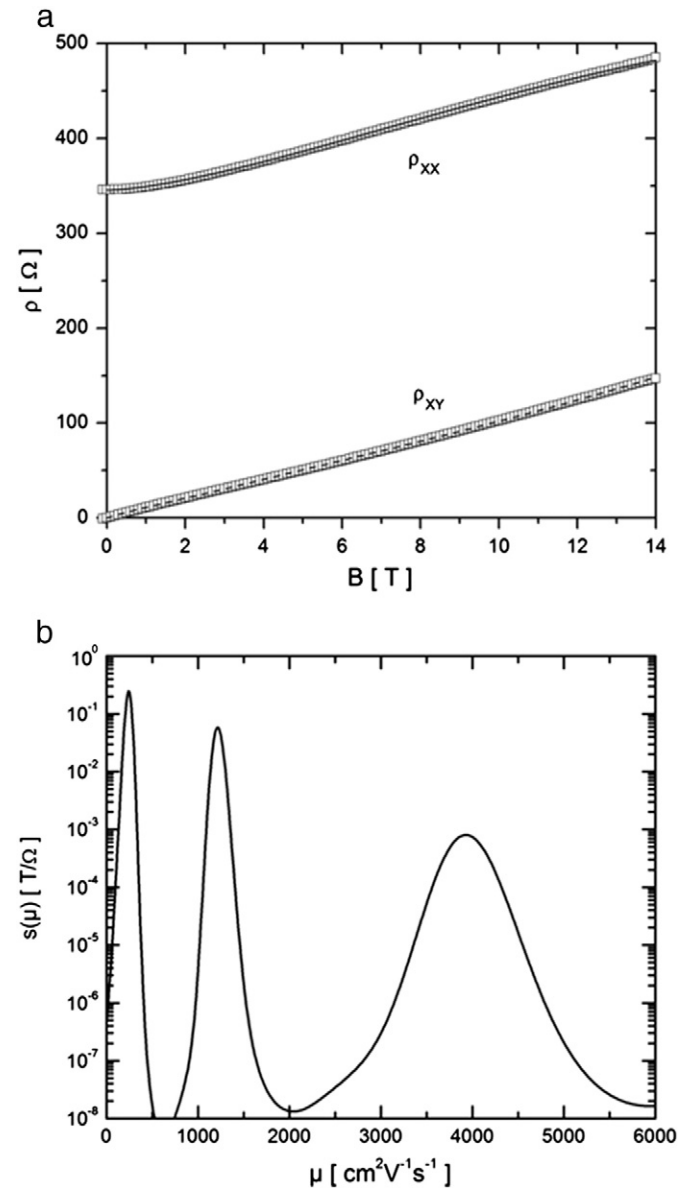


Fig. 6. (a) Magnetoresistance ρ_{xx} and Hall resistance ρ_{xy} as function of magnetic field (B) for 11-289-SQ1 and (b) mobility spectrum simulation at 300 K using BAMS for 11-289-SQ1.

the measured LT Hall sheet density where all parallel conduction is frozen out. A potential explanation for this is that for a sGe QW the RT Fermi level moves away from the Ge valence band as a result of strong ionization of boron impurities [4,5,23].

2.3. Bryan's algorithm mobility spectrum analysis (BAMS)

The 2 dimensional hole gas (2DHG) mobility in the sGe QW was also extracted from the magnetoresistance data using a different methodology, namely the Bryan's algorithm mobility spectrum (BAMS) technique [20]. The RT mobility spectrum obtained from BAMS is shown in Fig. 6 where the channel mobility is once again determined to be almost $4000 \text{ cm}^2/\text{V s}$. The carrier density is found to be lower using this technique ($5.9 \times 10^{10} \text{ cm}^{-2}$) and therefore the sample conduction at RT is again dominated by two low-mobility peaks with the channel only accounting for $\sim 1\%$. At 100 K (Fig. 7), the sGe QW mobility increases to $28,400 \text{ cm}^2/\text{V s}$ and carrier density to $3.1 \times 10^{11} \text{ cm}^{-2}$. At this temperature the parallel conduction begins to freeze out and so the channel now represents $\sim 80\%$ of the total conductivity. In Fig. 3 the results are

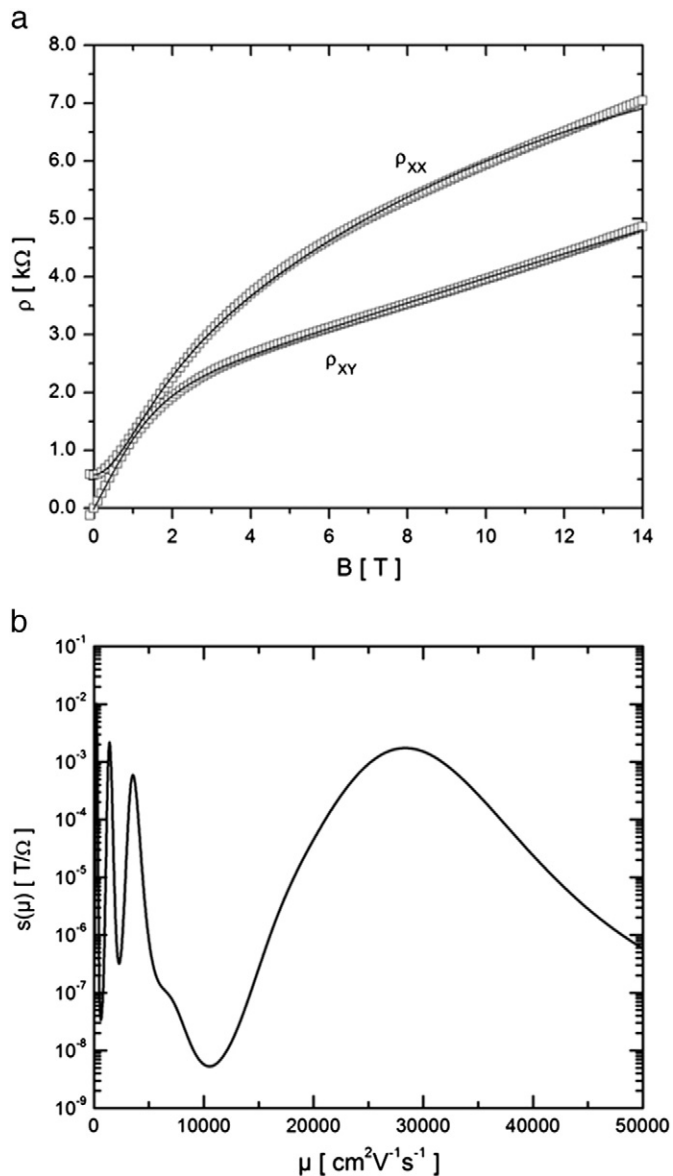


Fig. 7. (a) Magnetoresistance ρ_{xx} and Hall resistance ρ_{xy} as function of magnetic field (B) at 100 K, comparing data (squares) and the fit obtained by a forward-transform of the extracted mobility spectrum, for normal structure 11-289-SQ1 and (b) mobility spectrum at 100 K using BAMS for 11-289-SQ1.

Table 1

Mobility and sheet density results extracted using ME-MSA and BAMS.

Temperature (K)	p_s ($\times 10^{11} \text{ cm}^{-2}$) BAMS	p_s ($\times 10^{11} \text{ cm}^{-2}$) ME-MSA	μ ($\text{cm}^2/\text{V s}$) BAMS	μ ($\text{cm}^2/\text{V s}$) ME-MSA
50	3.15	2.93	$(4.5 \pm 1.5) \times 10^5$	$(2.3 \pm 0.5) \times 10^5$
100	3.05	2.88	$(2.8 \pm 0.4) \times 10^4$	$(3.0 \pm 0.4) \times 10^4$
150	1.96	2.38	$(1.1 \pm 0.1) \times 10^4$	$(1.1 \pm 0.3) \times 10^4$
200	1.47	1.71	$(6.7 \pm 0.4) \times 10^3$	$(6.3 \pm 1.3) \times 10^3$
300	0.59	0.98	$(3.9 \pm 0.2) \times 10^3$	$(3.9 \pm 0.4) \times 10^3$

compared with the Hall effect measurements taken using the Van der Pauw method as well as the ME-MSA results. Although the Hall bar with a width of $50 \mu\text{m}$ and a probe arm separation of either 250 or $500 \mu\text{m}$ shows the highest mobility at 12 K for this sample, the ME-MSA and BAMS analysis had to be carried out using the Van der Pauw square sample because of the current leakage around HB mesa. Both the ME-MSA and BAMS techniques revealed three peaks for holes in the sample, one being attributable to the holes in the channel while the other two are believed to correspond to a boron spike in the 2 nm Si cap and the 13 nm doping layer with an average concentration of $1.4 \times 10^{18} \text{ cm}^{-2}$ as determined from the uleSIMS depth profile of Fig. 2. Table 1 shows the 2D hole mobilities for different temperatures obtained by the two approaches i.e. ME-MSA and BAMS.

3. Conclusion

In this paper the RT 2DHG drift and Hall mobilities have been investigated for a pure sGe QW channel. The measured RT Hall mobility was found to be $1347 \text{ cm}^2/\text{V s}$ while the combined layer sheet density was $p_s^* = 1.27 \times 10^{13} \text{ cm}^{-2}$. Using two independent mathematical extraction techniques, ME-MSA and BAMS, the sGe channel drift mobility and sheet density from 50 K up to RT were determined. The RT values were $(3.9 \pm 0.4) \times 10^3 \text{ cm}^2/\text{V s}$ ($p_s = 9.8 \times 10^{10} \text{ cm}^{-2}$) using ME-MSA and $(3.9 \pm 0.2) \times 10^3 \text{ cm}^2/\text{V s}$ ($p_s = 5.9 \times 10^{10} \text{ cm}^{-2}$) using BAMS. These mobilities represent the highest RT values found to date for sGe.

Acknowledgment

This work has been partially supported by the EPSRC UK Renaissance Germanium project, by EuroMagNET under EU contract No. 228043, by HLD at HZDR, member of the European, Magnetic Field Laboratory (EMFL), by Slovak Research and Development Agency under the contract Nos. APVV-0132-11 and VEGA-0106-13, and SAS Centre of Excellence CFNT MVEP. OAM acknowledged the National Scholarship Program of the Slovak Republic for the Mobility Support for Researchers in the Academic Year 2012/2013. Part of this work was supported by DFG project DR832/3-1.

References

- [1] A. Dobbie, M. Myronov, R.J.H. Morris, A.H.A. Hassan, M.J. Prest, V.A. Shah, E.H.C. Parker, T.E. Whall, D.R. Leadley, Appl. Phys. Lett. 101 (17) (2012) 172108.
- [2] K. Sawano, Y. Abe, H. Satoh, Y. Shiraki, K. Nakagawa, Appl. Phys. Lett. 87 (19) (2005) 192102.
- [3] B. Rossner, D. Chrastina, G. Isella, H. von Kanel, Appl. Phys. Lett. 84 (16) (2004) 3058.
- [4] B. Rossner, H. von Kanel, D. Chrastina, G. Isella, B. Batlogg, Thin Solid Films 508 (1–2) (2006) 351.
- [5] M. Myronov, A. Dobbie, V.A. Shah, X.C. Liu, V.H. Nguyen, D.R. Leadley, Electrochem. Solid-State Lett. 13 (11) (2010) H388.
- [6] S. Madhavi, V. Venkataraman, Y.H. Xie, Appl. Phys. Lett. 89 (2001) 2497.
- [7] T. Tanaka, Y. Hoshi, K. Sawano, N. Usami, Y. Shiraki, K.M. Itoh, Appl. Phys. Lett. 100 (2012) 222102.
- [8] T. Irisawa, S. Tokumitsu, T. Hattori, K. Nakagawa, S. Koh, Y. Shiraki, Appl. Phys. Lett. 81 (5) (2002) 847.
- [9] T. Irisawa, H. Miura, T. Ueno, Y. Shiraki, Jpn. J. Appl. Phys. 40/4B (2001) 2694.
- [10] R.J.H. Morris, T.J. Grasby, R. Hammond, M. Myronov, O.A. Mironov, D.R. Leadley, T.E. Whall, E.H.C. Parker, M.T. Currie, C.W. Leitz, E.A. Fitzgerald, Semicond. Sci. Technol. 19 (10) (2004) L106.
- [11] M. Myronov, K. Sawano, K.M. Itoh, Y. Shiraki, Appl. Phys. Express 1 (5) (2008) 3.

- [12] H. von Kanel, D. Chrastina, B. Rossner, G. Isella, J.P. Hague, M. Bollani, *Microelectron. Eng.* 76 (1–4) (2004) 279.
- [13] M. Myronov, T. Irisawa, O.A. Mironov, S. Koh, Y. Shiraki, T.E. Whall, E.H.C. Parker, *Appl. Phys. Lett.* 80 (17) (2002) 3117.
- [14] H. von Kanel, M. Kummer, G. Isella, E. Muller, T. Hackbarth, *Appl. Phys. Lett.* 80 (16) (2002) 2922.
- [15] M. Myronov, Y. Shiraki, T. Mouri, K.M. Itoh, *Appl. Phys. Lett.* 90 (19) (2007) 192108.
- [16] M. Myronov, X.C. Liu, A. Dobbie, D.R. Leadley, *J. Cryst. Growth* 318 (1) (2011) 337.
- [17] G. Hock, M. Gluck, T. Hackbarth, H.J. Herzog, E. Kohn, *Thin Solid Films* 336 (1998) 141.
- [18] D.R. Leadley, V.V. Andrievskii, I.B. Berkutov, Y.F. Komnik, T. Hackbarth, O.A. Mironov, *J. Low Temp. Phys.* 159 (1–2) (2010) 230.
- [19] S. Kiatgamolchai, M. Myronov, O.A. Mironov, V.G. Kantser, E.H.C. Parker, A.T.E. Whall, *Phys. Rev. E* 66 (2002) 036705.
- [20] D. Chrastina, J.P. Hague, D.R. Leadley, *J. Appl. Phys.* 94 (10) (2003) 6583.
- [21] G. Capellini, M.D. Seta, Y. Busby, M. Pea, F. Evangelisti, G. Nicotra, C. Spinella, M. Nardone, C. Ferrari, *J. Appl. Phys.* 107 (6) (2010) 063504.
- [22] V.A. Shah, A. Dobbie, M. Myronov, D.R. Leadley, *J. Appl. Phys.* 107 (6) (2010) 064304.
- [23] A. Dobbie, V.H. Nguyen, R.J.H. Morris, X.-C. Liu, M. Myronov, D.R. Leadley, *J. Electrochem. Soc.* 159 (5) (2012) H490.
- [24] A.H.A. Hassan, O.A. Mironov, A. Dobbie, J.H. Morris, J.E. Halpin, V.A. Shah, M. Myronov, D.R. Leadley, S. Gabani, A. Feher, E. Cizmar, V.V. Andrievskii, I.B. Berkutov, IEEE XXXIII International Scientific Conference, 16–19 April, *Electron. Nanotechnol (ELNANO)*, 51, 2013, p. 55, (2013).
- [25] R.J.H. Morris, M.G. Dowsett, R. Beanland, A. Dobbie, M. Myronov, D.R. Leadley, *Anal. Chem.* 84 (5) (2012) 2292.
- [26] S.-H. Huang, T.-M. Lu, S.-C. Lu, C.-H. Lee, C.W. Liu, D.C. Tsui, *Appl. Phys. Lett.* 101 (4) (2012) 042111.